Hydrogen-related defects and the role of metal additives in the kinetics of complex hydrides: A first-principles study

Khang Hoang and Chris G. Van de Walle*
Materials Department, University of California, Santa Barbara, California 93106-5050, USA
(Received 30 July 2009; revised manuscript received 5 November 2009; published 11 December 2009)

We report first-principles studies of hydrogen-related point defects and impurities in $LiBH_4$ and $Li_4BN_3H_{10}$, two promising materials for hydrogen storage. In both systems, hydrogen vacancies and interstitials are found to be positively or negatively charged, and hence their formation energies are Fermi-level dependent. One can therefore tailor the formation energies of these point defects (hence the kinetics of the systems) by shifting the Fermi level. This can be accomplished by adding appropriate impurities that are electrically active into the systems. We have identified a number of transition-metal impurities that are effective in shifting the Fermi level of $LiBH_4$ and $Li_4BN_3H_{10}$. A comparison of our calculations with experimental results for the effects of addition of impurities on the kinetics of $LiBH_4$ and $Li_4BN_3H_{10}$ shows qualitative agreement, providing validation for our interpretation of the results and for our proposed model for enhancement of kinetics.

DOI: 10.1103/PhysRevB.80.214109 PACS number(s): 71.20.Ps, 61.50.Lt, 66.30.Lw

I. INTRODUCTION

As fossil fuel supplies decrease and world demands for energy increase, one of the biggest challenges that will face humankind in the 21st century is to provide a sustainable supply of energy to the world's population. Hydrogen, which can serve as an energy carrier in a carbon-neutral system of energy production and use, is expected to play an increasingly important role in meeting these challenges.[1,2] Although hydrogen storage materials have exhibited significant improvements in recent years in terms of weight capacity, reversibility, and kinetics, major advances are still needed in order to meet future requirements. First-principles calculations based on density-functional theory can act as an important tool in supporting such progress.[3]

Recently, complex hydrides such as $LiBH_4$ and $Li_4BN_3H_{10}$ (synthesized from $LiBH_4/LiNH_2$ mixtures) have been identified as promising hydrogen storage materials. These borohydrides, however, exhibit limitations in kinetics and/or reversibility.[4,5] $LiBH_4$, for instance, has high hydrogen density (18.5 wt %) but high thermodynamic stability and slow kinetics.[4] $Li_4BN_3H_{10}$, on the other hand, has theoretical hydrogen content of 11.9 wt % and releases greater than 10 wt % hydrogen when heated,[5] but rehydrogenation may be thermodynamically unfavorable.[6] Accurate modeling of hydrogen kinetics in these systems is essential for developing a more complete understanding of the processes that limit the performance of storage materials, and ultimately, for the development of improved materials systems.

In this work, we perform first-principles studies for $LiBH_4$ and $Li_4BN_3H_{10}$ with a focus on the processes that govern the addition, removal, and diffusion of individual hydrogen atoms, and the effects of metal additives on such processes. Hydrogen is treated as an "impurity" in the materials and hydrogen-related point defects such as vacancies and interstitials are investigated. One of the key findings is that hydrogen-related defects are charged and their formation energies are, therefore, Fermi-level dependent. From a materials design perspective, this opens up an opportunity to tailor the formation energies (hence the concentrations) of hydrogen-related defects by shifting the Fermi level, as found to be effective in $NaAlH_4$.[7] This can be done by adding appropriate electrically active impurities into the systems.

Experimentally, it has been reported that metal additives such as $TiCl_3$, TiF_3, and ZnF_2 effectively reduce the dehydrogenation temperature of $LiBH_4$.[8] $LiBH_4$ ball milled with TiO_2 was also reported to dehydrogenate at much lower temperatures than as-received commercial $LiBH_4$.[9] In $Li_4BN_3H_{10}$, metal additives such as $NiCl_2$, Pd (or $PdCl_2$), and Pt (or $PtCl_2$) were found to drastically enhance the kinetics of the system.[6,10] On the other hand, some metal additives were also found not to be effective, such as $FeCl_3$ and a number of other halides in $LiBH_4$.[8] The addition of $TiCl_3$, Fe, Zn, and $ZnCl_2$ was found not to significantly improve dehydrogenation of $Li_4BN_3H_{10}$.[6,10]

Although a number of effective (as well as ineffective) metal additives have been identified experimentally, the role played by these additives is not fully understood. In order to investigate these issues, we have carried out an exploratory investigation of the interactions between different impurities and the host materials $LiBH_4$ and $Li_4BN_3H_{10}$. Transition metals such as Ti, Zr, Fe, Ni, Pd, Pt, and Zn were chosen for this purpose. Although some of these metals and/or their halides were experimentally found not to be effective in $LiBH_4$ and/or $Li_4BN_3H_{10}$, understanding the effects of all these impurities in the systems may help provide insight into the factors that govern enhancement of kinetics.

The arrangement of this paper is as follows: in Sec. II we provide methodological details of our first-principles calculations for defects and impurities. Bulk properties of $LiBH_4$ and $Li_4BN_3H_{10}$ are briefly discussed in Sec. III. In Secs. IV and V, we present our results for hydrogen-related point defects and transition-metal impurities. Possible correlation between our theoretical results and available experimental data is discussed in Sec. VI. We conclude the paper with a summary in Sec. VII.

II. METHODOLOGY

A. Formation energy

The formation energy of a defect X in charge state q is defined as[11]

$$E^f(X^q) = E_{tot}(X^q) - E_{tot}(\text{bulk}) - \sum_i n_i\mu_i + q(E_V + \mu_e), \quad (1)$$

where $E_{tot}(X^q)$ and $E_{tot}(\text{bulk})$ are, respectively, the total energies of a supercell containing X and of a supercell containing only bulk materials; μ_i is the chemical potential of species i (host atoms or impurity atoms), and n_i denotes the number of atoms of species i that have been added ($n_i>0$) or removed ($n_i<0$) to create the defect or impurity. μ_e is the chemical potential of electrons (Fermi energy) and E_V is the energy of the bulk valence-band maximum which we use as the reference for the Fermi energy. The chemical potentials μ_i can be rewritten as $\mu_i=\mu_i^0+\Delta\mu_i$, where μ_i^0 equals the chemical potential of element i in its standard state.

The decomposition process in $LiBH_4$ can proceed as $LiBH_4 \rightarrow LiH+B+3/2H_2$. We therefore assume equilibrium with LiH and B, and the chemical potentials of Li, B, and H in $LiBH_4$ can then be obtained from the equations that express the stability of LiH, B, and $LiBH_4$.[11] In $Li_4BN_3H_{10}$, one of the possible decomposition pathways is $Li_4BN_3H_{10} \rightarrow Li_3BN_2+\frac{1}{2}Li_2NH+\frac{1}{2}NH_3+4H_2$.[12] The chemical potentials of Li, B, N, and H in $Li_4BN_3H_{10}$ can be obtained by assuming equilibrium with Li_3BN_2, Li_2NH, and NH_3. For the impurities (Ti, Zr, Fe, Ni, Pd, Pt, and Zn), the chemical potentials are fixed to the energy of the bulk metals, i.e., $\Delta\mu_i=0$. One can, of course, choose a different set of chemical potentials and this may affect the relative formation energy between different types of impurities. These formation energies could easily be obtained from the data we report. However, this choice should not alter the physics of what we are presenting here.

The formation energy of a defect is a crucial factor in determining defect concentration. In thermal equilibrium, the concentration of the defect X at temperature T can be obtained via the relation[11]

$$c(X) = N_{\text{sites}}N_{\text{config}} \exp[-E^f(X)/kT], \quad (2)$$

where N_{sites} is the number of high-symmetry sites in the lattice per volume unit on which the defect can be incorporated and N_{config} is the number of equivalent configurations (per site) in which the defect can be formed. For charged defects, the concentrations are not independent but coupled by the condition of charge neutrality.

Equation (2) strictly speaking only applies in thermal equilibrium. For hydrogen-related defects, which have low migration barriers and can therefore readily equilibrate, this assumption is expected to be valid. For the transition-metal impurities, we do not expect equilibrium conditions to be satisfied, and incorporation will more likely be governed by kinetic limitations. However, even in that case the calculated formation energies provide useful information about the relative stability of different configurations, i.e., which site(s) will be more favorable.

Throughout this paper we will refer to $\varepsilon(q_1/q_2)$ as the thermodynamic transition level which is defined as the Fermi-level position where the charge states q_1 and q_2 have equal formation energy. From Eq. (1), it can be shown that the Fermi level at which the transition takes place is

$$\varepsilon(q_1/q_2) = \frac{1}{q_2-q_1}[E_{tot}(X^{q1}) - E_{tot}(X^{q2}) + (q_1-q_2)E_V], \quad (3)$$

where q_1 and q_2 are the initial and final charge states, respectively. The transition level would be observed in experiments if the final charge state can fully relax to its equilibrium configuration after the transition. This quantity will be used to characterize different impurities.

B. Calculational details

Structural optimization and total energy and electronic-structure calculations for $LiBH_4$ and $Li_4BN_3H_{10}$ were performed based on density-functional theory, using the generalized-gradient approximation (GGA) (Ref. 13) and the projector-augmented wave (PAW) (Refs. 14 and 15) method as implemented in the VASP code.[16–18] We treated the outermost s electrons (H and Li) or s and p electrons (B and N) of the constituent elements as valence electrons and the rest as core electrons, using the standard PAW potentials in the VASP database.

Calculations for bulk $LiBH_4$ (orthorhombic phase; 24 atoms/unit cell) were carried out using a $6\times10\times6$ Monkhorst-Pack[19] **k**-point mesh; for bulk $Li_4BN_3H_{10}$ (144 atoms/unit cell), we used a $2\times2\times2$ **k**-point mesh. For calculations of hydrogen-related defects and impurities, we used a $(2\times2\times2)$ supercell containing 192 atoms in the case of $LiBH_4$ or the unit cell of 144 atoms in the case of $Li_4BN_3H_{10}$, and a $2\times2\times2$ **k**-point mesh. The energy cutoff was set to 400 eV and convergence with respect to self-consistent iterations was assumed when the total energy difference between cycles was less than 10^{-4} eV and the geometry relaxation tolerance was better than 0.01 eV/Å.

III. BULK PROPERTIES

We first carried out calculations for bulk $LiBH_4$ and $Li_4BN_3H_{10}$ to extract basic information about the systems. The relaxed structures of $LiBH_4$ and $Li_4BN_3H_{10}$ are shown in Figs. 1(a) and 1(b) with H1, H2, H3, and H4 labeling the inequivalent hydrogen atoms. The calculated lattice parameters are $a=7.2477$ Å, $b=4.3910$ Å, and $c=6.6064$ Å for orthorhombic $LiBH_4$, and $a=10.85$ Å for cubic $Li_4BN_3H_{10}$; in satisfactory agreement with experimental values.[20,21] Our results for structural properties are comparable to those obtained in previous studies of $LiBH_4$ and $Li_4BN_3H_{10}$.[12,22–24]

Figures 2 and 3 show the total and partial density of states (DOS) for $LiBH_4$ and $Li_4BN_3H_{10}$. In $LiBH_4$, the valence-band maximum (VBM) is dominated by bonding states consisting of B p and H s states, whereas the conduction-band minimum (CBM) consists predominantly of the antibonding state of B p and H s states plus contributions from Li s states. In $Li_4BN_3H_{10}$, there are unbonded states (lone pairs) coming from N in NH_2 units. These unbonded N p states are higher in energy than B p states and predominantly contribute to the VBM. Electronic states coming from N s are very deep in the energy spectrum, about 15 eV below the Fermi level. The CBM of $Li_4BN_3H_{10}$ consists predominantly of N p states. Li s states appear in a wide range of energies, in both valence band and conduction band. The electronic

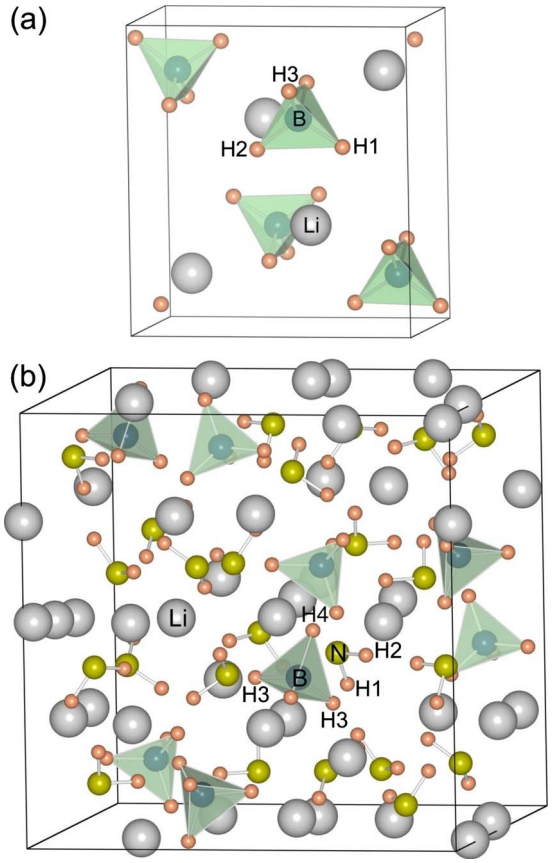

FIG. 1. (Color online) Relaxed structures of (a) $LiBH_4$ and (b) $Li_4BN_3H_{10}$. Large (gray) spheres are Li, medium (blue) spheres B, small (green) spheres N, and smaller (orange) spheres H. Inequivalent hydrogen atoms are labeled as H1, H2, H3, and H4.

structure of $Li_4BN_3H_{10}$ in the band-gap region is, therefore, dominated by that of $LiNH_2$, as confirmed by calculations for $LiNH_2$ in which we observe similar characteristics. Our results for the DOS of $LiBH_4$ and $Li_4BN_3H_{10}$ are in qualitative agreement with those reported in previous work.[12,21,23]

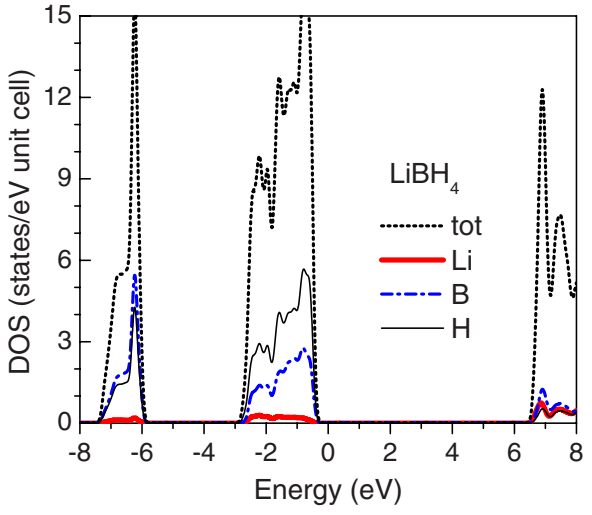

FIG. 2. (Color online) Total and partial densities of states (DOS) for $LiBH_4$. The zero of energy is set to the highest-occupied state.

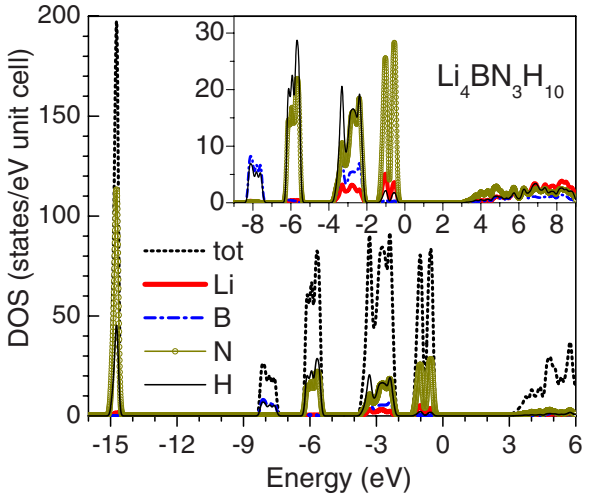

FIG. 3. (Color online) Total and partial densities of states (DOS) for $Li_4BN_3H_{10}$. The zero of energy is set to the highest-occupied state. The inset enlarges the partial DOS curves.

The calculated band gaps (within GGA) of $LiBH_4$ and $Li_4BN_3H_{10}$ are, respectively, 7.01 and 3.53 eV; both are direct gaps at the Γ point. For comparison, Miwa *et al.*[23] reported a band gap of 6.8 eV for $LiBH_4$, and Herbst and Hector[12] and Yang *et al.*[21] reported a band gap of about 4 and 2.7 eV for $Li_4BN_3H_{10}$, respectively. Experimental information about the band gap of these two compounds is not yet available, to our knowledge. Considering only the total energies, the formation enthalpies (at $T=0$ K) with respect to the elemental constituents are −192.79 kJ/mol for $LiBH_4$ and −799.11 kJ/mol for $Li_4BN_3H_{10}$. Vibrational properties are not addressed in this paper but could be included based on formalisms discussed, e.g., in Ref. 25. The above values are comparable to those obtained by Siegel *et al.*,[22] namely, −205.90 and −806.90 kJ/mol.

IV. HYDROGEN-RELATED DEFECTS

We investigated hydrogen interstitials (H_i) and hydrogen vacancies (V_H) in all three possible charge states (+1, 0, and −1) and at different positions (V_H nominally on inequivalent H sites and H_i at different interstitial locations) in both $LiBH_4$ and $Li_4BN_3H_{10}$. Formation energies of the defects were obtained using the method described in Sec. II.

A. $LiBH_4$

Figure 4 shows the formation energies of the lowest-energy configurations of hydrogen vacancies and hydrogen interstitials in $LiBH_4$. For both cases, hydrogen-related charged defects are energetically more favorable than neutral ones over the entire range of Fermi-level values, which is a characteristic of systems with negative correlation energy U.[26] The defects with lowest formation energy are V_H^+ (initially created on the H3 site) and H_i^- (initially placed near the center of the void formed by Li atoms and BH_4 units).

In insulators such as $LiBH_4$ and $NaAlH_4$, the condition of charge neutrality can be fulfilled by having equal concentra-

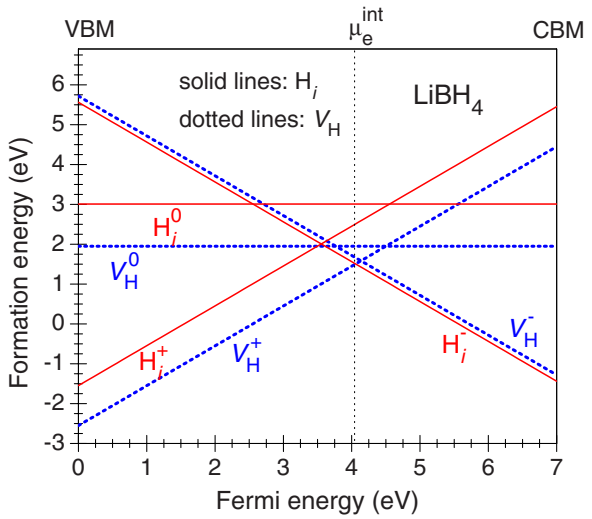

FIG. 4. (Color online) Calculated formation energies of hydrogen-related defects (V_H and H_i) in $LiBH_4$ as a function of Fermi energy. Only the formation energies of the lowest-energy configurations are shown. V_H^0 and V_H^+ were initially created on the H3 site and V_H^- initially on the H1 site [see Fig. 1(a) for definition of H1 and H3 sites]. H_i^0 and H_i^+ were initially placed near the midpoint of the B-B bond, and H_i^- initially near the center of the void formed by Li atoms and BH_4 units.

tions of defects with opposite charges.[7] Different defects exist in the system with different concentrations. However, the ones with the lowest formation energy have the highest concentrations and are dominant. Figure 4 indicates that, in the absence of extrinsic impurities, the Fermi level will be at $\mu_e^{int}=4.06$ eV, where the formation energies (and hence, approximately, the concentrations) of intrinsic point defects V_H^+ and H_i^- are equal. This value is obtained with respect to the chosen set of chemical potentials.

There are significant changes in the lattice geometry of $LiBH_4$ in the presence of hydrogen-related defects; this is why in the descriptions of geometry above we focus on the *initial* placement (nominal position) of the defect, since after relaxation the structures tend to become a lot more complicated. For example, the creation of a neutral hydrogen vacancy (V_H^0) by removing one hydrogen atom from a BH_4 unit turns this tetrahedral complex into a trigonal planar BH_3 unit (essentially a BH_3 molecule). V_H^+ leads to formation of a BH_3-H-BH_3 complex (two BH_4 units that share a common H atom); see Fig. 5(a). V_H^-, finally, leads to formation of a BH_3 unit.

We also see different relaxation patterns associated with hydrogen interstitials created in different charge states in the lattice geometry of $LiBH_4$. The creation of H_i^0 results in a trigonal planar BH_3 complex plus an H_2 molecule. H_i^+ similarly results in a BH_3 unit plus an H_2 molecule but could, alternatively, be described as a BH_5 complex; see Fig. 5(b). This pattern of lattice relaxations is different from what was observed in $NaAlH_4$ where the creation of H_i^+ leaves the system with an AlH_3-H-AlH_3 complex and an H_2 molecule.[7] In fact, a pattern similar to that of $NaAlH_4$, namely, a BH_3-H-BH_3 complex and an H_2 molecule, was also found for H_i^+ in $LiBH_4$, however it is 0.15 eV higher in energy than

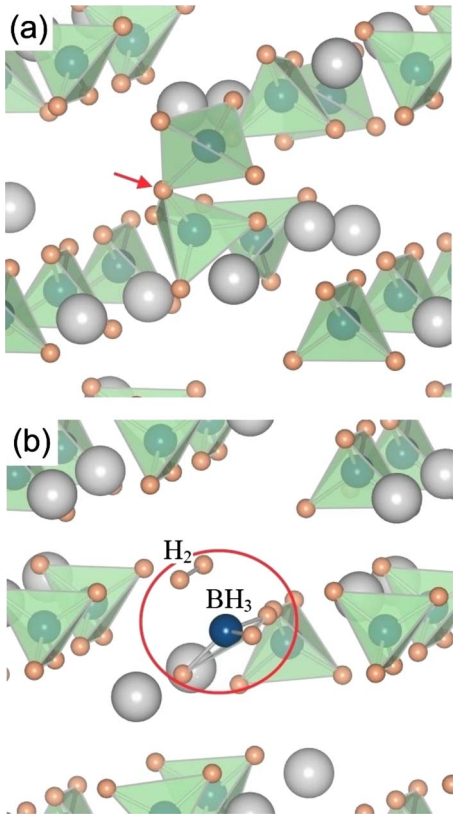

FIG. 5. (Color online) Lattice relaxations induced by (a) a positively hydrogen vacancy V_H^+ and (b) a positively hydrogen interstitial H_i^+ in $LiBH_4$. Large (gray) spheres are Li, medium (blue) spheres B, and small (orange) spheres H. The removal of one hydrogen atom and one electron from a BH_4 unit to form V_H^+ leads to formation of one BH_3-H-BH_3 complex (two BH_4 units that share a common H atom; marked by the arrow), whereas the creation of H_i^+ leaves the system with a BH_3 unit and an H_2 molecule (marked by the circle).

lowest-energy configuration described above.

H_i^- in $LiBH_4$, on the other hand, does not break any BH_4 unit but is located in the interstitial void, next to two Li atoms (a Li-H-Li unit with the Li-H distances being 1.76 and 1.78 Å). This is also different from what was observed for H_i^- in $NaAlH_4$, where an AlH_5 complex and a distorted AlH_4 tetrahedron (alternately viewed as an AlH_4-H-AlH_4 complex) were found.[7]

We suggest that the BH_3 units observed in the case of V_H^- and H_i^+ could combine and form diborane (B_2H_6) which may be emitted during the dehydrogenation process. This may account for the unrecoverable loss of boron reported in experiment.[8]

In addition to creating different patterns in the local bonding characteristics of $LiBH_4$, these hydrogen-related point defects strongly disturb the neighboring region by moving and/or rotating other Li atoms and BH_4 units. Significant changes in the lattice geometry, especially those associated with positively charged hydrogen vacancies (V_H^+) or interstitials (H_i^+), explain why neutral hydrogen-related defects in $LiBH_4$ are not stable energetically and decay into charged defects (a characteristic of negative-U systems).

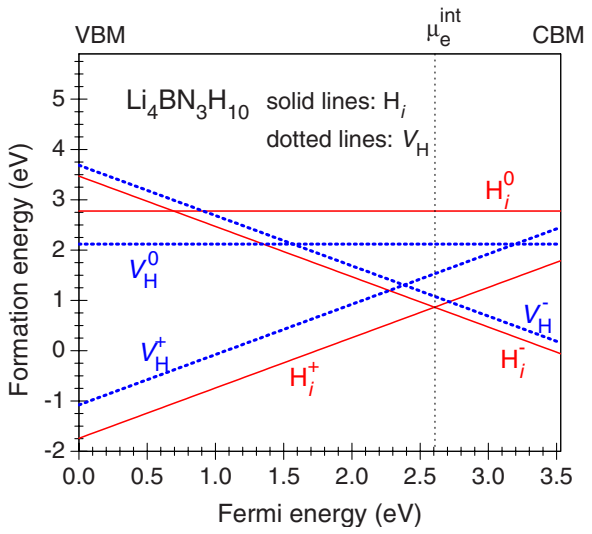

FIG. 6. (Color online) Calculated formation energies of hydrogen-related defects in $Li_4BN_3H_{10}$ as a function of Fermi energy. Only the formation energies of the lowest-energy configurations are shown. V_H^0 and V_H^+ were initially created on the H3 site, and V_H^- initially on the H2 site [see Fig. 1(b) for definition of H2 and H3 sites]. H_i^0, H_i^+, and H_i^- were initially placed at various different locations, as described in the text.

We note that Łodziana *et al.*[27] have reported first-principles calculations for native point defects in $LiBH_4$ using a methodology similar to ours. However, there are unexplained discrepancies between our results and those of Łodziana *et al.* The transition level $\varepsilon(+/-)$ between the + and − charge states of the hydrogen vacancy and hydrogen interstitial occurs at much lower values in the band gap than it does in our calculations. For example, $\varepsilon(+/-)$ for hydrogen vacancy is ~0.25 eV in Łodziana *et al.* whereas it is 4.14 eV in ours; the difference (~3.9 eV) is comparable to the energy of the valence-band maximum of the bulk (3.5 eV) in our calculations, which could indicate an error in the reference energy for the Fermi level.

B. $Li_4BN_3H_{10}$

Figure 6 shows the formation energies of hydrogen vacancies and hydrogen interstitials in $Li_4BN_3H_{10}$, in their lowest-energy configurations. Like in $LiBH_4$, hydrogen-related charged defects in $Li_4BN_3H_{10}$ are energetically more favorable than neutral ones over the entire range of Fermi-level values. However, unlike $LiBH_4$, the two lowest formation energy defects in $Li_4BN_3H_{10}$ are of the same type: H_i^+ and H_i^-. In the absence of extrinsic impurities, the Fermi level will be at μ_e^{int}=2.61 eV where the formation energies of H_i^+ and H_i^- are equal.

We note that the formation energies of hydrogen-related defects in $Li_4BN_3H_{10}$ are quite low; in fact, lower than the calculated values in $NaAlH_4$ (Ref. 6) or $LiBH_4$ (Fig. 4). With such low formation energies, there can be no doubt that these defects play a role in the decomposition kinetics of $Li_4BN_3H_{10}$.

We observed remarkable changes induced by hydrogen-related defects in the lattice geometry of $Li_4BN_3H_{10}$. V_H^0 is most stable when it is created by removing a hydrogen atom from the H3 site in a BH_4 unit; this leaves the system with a trigonal planar BH_3 complex. For V_H^+, a BH_3-H-BH_3 complex (two BH_4 complexes sharing a common hydrogen atom) is formed when a hydrogen atom is removed from the H3 site, which is similar to what we observed for V_H^+ in $LiBH_4$. V_H^-, on the other hand, is most stable when created on the H2 site, i.e., by removing one hydrogen atom from an NH_2 unit; this leaves the system with a NH unit.

As for hydrogen interstitials in $Li_4BN_3H_{10}$, H_i^0 is most stable when the interstitial hydrogen comes near a BH_4 unit and loosely bonds with one of the four hydrogen atoms in the unit. The lowest-energy configuration of H_i^+ is obtained when this positively charged hydrogen interstitial combines with an NH_2 unit to form an NH_3 molecule. The formation energy of H_i^+ is very small in this case, much smaller than that of V_H^+ (see Fig. 6), which is a distinctive feature of $Li_4BN_3H_{10}$ compared to $LiBH_4$. The formation of NH_3 molecules, which could be emitted during the dehydrogenation process, may explain the observed NH_3 release in experiment.[5] Finally, H_i^- is most stable situated in the void formed by Li, BH_4, and NH_2 species and has two Li atoms as the nearest neighbors with the Li-H distances being 1.80 and 1.81 Å. This is similar to what we have observed for H_i^- in $LiBH_4$. All these examples of lattice relaxations in $Li_4BN_3H_{10}$ (and also in $LiBH_4$) show that hydrogen-related point defects create large lattice relaxations that can potentially serve as nucleation sites for new phases during the dehydrogenation process.

C. Diffusion of hydrogen-related point defects

We have investigated the diffusion path of hydrogen vacancies and interstitials in $LiBH_4$ and $Li_4BN_3H_{10}$ and estimated the energy barriers for diffusion using the climbing image nudged elastic band method (CI-NEB).[28] The migration path of hydrogen interstitials was calculated by sampling hydrogen positions between ground-state configurations. The migration barrier is the energy difference between the saddle point and the ground state. For vacancies, the path is calculated by moving a hydrogen atom from a nearby lattice site into the vacancy. All the CI-NEB calculations were performed with the VASP code.[16–18] Our results show that the migration barriers of H_i^+ and H_i^- are 0.65 and 0.60 eV in $LiBH_4$, and 0.48 and 0.49 eV in $Li_4BN_3H_{10}$, respectively. The migration barriers of hydrogen vacancies are higher than those of hydrogen interstitials; for example, our CI-NEB calculations give migration barriers of 1.32 eV for V_H^- in $LiBH_4$ and 0.65 eV for V_H^+ in $Li_4BN_3H_{10}$. The migration barrier for V_H^- in $LiBH_4$ is high because the saddle-point configuration consists of a hydrogen atom located midway between the two BH_3 units. Such a configuration (i.e., BH_3-H-BH_3) is favorable in the case of V_H^+ but high in energy in the case of V_H^-. All of the above results are upper bounds on the migration barrier. We note that explicit calculations for migration paths in these complex hydrides are very difficult because of the complexities of the lattice relaxations associated with the defects, which lead to huge demands on computing resources.

V. TRANSITION-METAL IMPURITIES

For an exploratory investigation of impurities in $LiBH_4$ and $Li_4BN_3H_{10}$, we carried out calculations for Ti, Zr, Fe, Ni,

TABLE I. Transition level $\varepsilon(+/-)$ between charge states +1 and −1, the associated U value, and the corresponding formation energy E^f (where U is negative) of different impurities nominally on the B and Li sites and at interstitial sites in $LiBH_4$. In cases where U is positive, E^f is the formation energy of impurities in the neutral charge state. Configurations that have positive U but may still be effective in shifting the Fermi level are marked with a $\surd$ sign, whereas ineffective configurations are marked with a × sign. Work functions (Φ) of the impurities in their metallic states are also given for reference. All the quantities are given in electron volt (eV). The transition level between V_H^+ and H_i^- (in their most stable configurations) is at μ_e^{int} =4.06 eV.

		Ti	Zr	Fe	Ni	Pd	Pt	Zn
	Φ[a]	4.10	4.00	4.65	5.15	5.00	5.40	4.30
B site	$\varepsilon(+/-)$	4.16	4.44	3.71	3.65	3.27	3.19	3.79
	U	−0.93	−1.46	−0.91	−2.02	−2.12	−1.61	−3.26
	E^f	3.90	2.99	2.95	2.67	2.69	1.92	2.78
	$\varepsilon(+/-)-\mu_e^{int}$	+0.10	+0.38	−0.35	−0.41	−0.79	−0.87	−0.27
Li site	$\varepsilon(+/-)$	4.37	4.60	4.08	3.33	3.04	3.16	4.03
	U	−0.32	−0.31	+0.72	+1.11	−0.01	−1.76	−1.75
	E^f	3.56	3.56	3.74	3.01	3.29	3.24	3.92
	$\varepsilon(+/-)-\mu_e^{int}$	+0.31	+0.54	×	$\surd$	−1.03	−0.90	−0.03
Interstitial	$\varepsilon(+/-)$	4.81	4.45	4.30	4.36	4.15	3.93	4.33
	U	−0.30	−0.33	+0.29	+2.53	+3.06	+3.20	+2.83
	E^f	3.90	3.97	3.54	1.85	1.55	1.82	2.11
	$\varepsilon(+/-)-\mu_e^{int}$	+0.75	+0.39	×	×	×	×	×

[a]Reference 29.

Pd, Pt, and Zn. Among the possible positions, the impurities can be nominally on the Li, B, and N sites, and at interstitial sites. For each type of substitutional or interstitial impurity, calculations were carried out in various configurations to be sure that the lowest-energy configurations are obtained. Indeed, we have found that the complexity of the lattice structures renders it quite common for a number of different metastable configurations to occur. Significant effort has to be devoted to make sure that the global minimum is identified.

A. $LiBH_4$

Table I summarizes the results for transition levels $\varepsilon(+/-)$ between charge states +1 and −1, the associated U value which is defined as $U=\varepsilon(0/-)-\varepsilon(+/0)$, and the corresponding formation energy E^f of the impurities on the B and Li sites and at interstitial sites in $LiBH_4$. We found that all the impurities nominally on the B site have negative correlation energy U. This can also be seen in Figs. 7(a)–7(d) where we plot formation energies for several representative impurities in various charge states (−2, −1, 0, +1, and +2) on the B site.

In the absence of other defects and impurities, the Fermi level would be fixed at the position shown in Fig. 4 (μ_e^{int} =4.06 eV), which ensures that positively and negatively charged defects occur in equal numbers and charge neutrality is obeyed. Now we examine what happens if transition-metal impurities, which are also electrically active, are introduced into the system. If the concentration of transition-metal impurities is larger than that of the hydrogen-related defects (which is quite plausible since typically several percents of the metallic impurity are added), the Fermi level of the system will now be determined by the transition-metal impurity. Chances are that this Fermi-level position will be different from the one that would occur in the absence of the impurity. An immediate consequence is that the formation energy of one of the hydrogen-related defects will be reduced (see Fig. 4). This mechanism, proposed by Peles and Van de Walle for $NaAlH_4$,[7] is expected to also be active in (de)hydrogenation

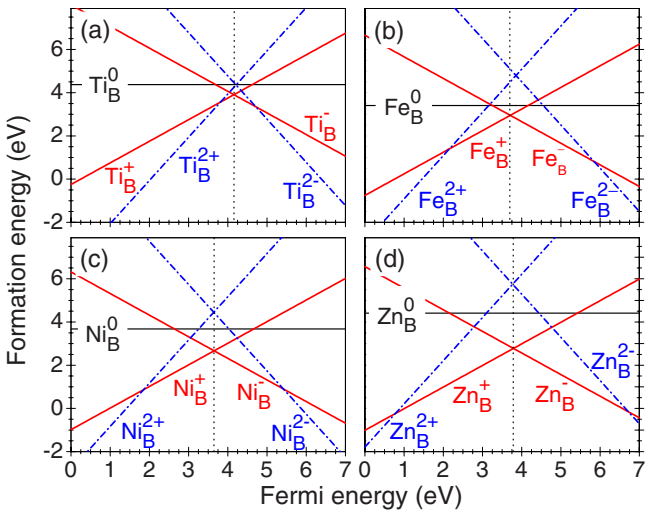

FIG. 7. (Color online) Calculated formation energies of (a) Ti, (b) Fe, (c) Ni, and (d) Zn nominally on the B site in $LiBH_4$. Other impurities (Zr, Pd, Pt, and Zn) have similar features. The vertical dashed line is $\varepsilon(+/-)$, the transition level between charge states +1 and −1 of the impurity.

of $LiBH_4$. The energy difference between $\varepsilon(+/-)$ and μ_e^{int} are different for different impurities. This may explain why some metal additives are more effective than others.

The case where the transition-metal impurity has negative-U character is relatively simple: if the impurity is present in larger concentrations than any other impurity or any point defects, it will dominate in the charge-neutrality equation and the Fermi level will simply coincide with the $\varepsilon(+/-)$ transition level of the impurity. For this reason we list this quantity in Table I. Many impurities located at interstitial sites and some impurities substituting on the Li site, however, do not have negative-U character.

For impurities that exhibit positive U, a shift in the Fermi level (away from μ_e^{int}) is still to be expected, but to establish the magnitude of that shift we need a slightly different analysis. Fermi-level positions are still obtained by imposing charge neutrality while taking account of all possible charge states of the impurity, as well as the presence of charged hydrogen-related defects. There are three possible scenarios in the positive-U case: (i) $\mu_e^{int} < \varepsilon(+/0)$, (ii) $\varepsilon(+/0) < \mu_e^{int} < \varepsilon(0/-)$, and (iii) $\mu_e^{int} > \varepsilon(0/-)$. In cases (i) and (iii), one can still get a significant shift of the Fermi level when the impurity is incorporated. Charge neutrality in (i) will be established by having equal numbers of positively charged transition-metal impurities and negatively charged hydrogen-related defects; in (iii), by having a balance between negatively charged transition-metal impurities and positively charged hydrogen-related defects. Only in (ii) will the transition-metal impurity have no effect (since it prefers the neutral charge state over a range of Fermi levels that includes the Fermi-level position where the hydrogen-related defects switch charge state).

Based on this analysis, we identified Ni_{Li} as a configuration that shows positive-U character but has $\mu_e^{int} > \varepsilon(0/-)$, and is thus possibly effective additive in $LiBH_4$. Others such as Fe_{Li}, Ni_i, Pd_i, Pt_i, and Zn_i, where $\varepsilon(+/0) < \mu_e^{int} < \varepsilon(0/-)$, and Fe_i, where $\varepsilon(+/0) \sim \mu_e^{int}$, are expected not to be effective in $LiBH_4$.

We note that our results for Ti are very different from those of Łodziana *et al.*[27] where it was reported that the neutral Ti impurity in $LiBH_4$ is energetically more favorable than charged ones over almost the entire range of Fermi-level values. We have no plausible explanation for the discrepancies.

Drastic changes occur in the lattice geometry of $LiBH_4$ in the presence of transition-metal (M) impurities, which can be even larger than the changes described for hydrogen-related defects. The impurities tend to pull BH_4 units closer and/or, in many cases, break B-H bonds to form MH_n complexes (M=Ti, Zr, Fe, Ni, Pd, Pt, and Zn). In the case of positively charged Pd, Pt, and Zn impurities on the B site, these rearrangements also create H_2 molecules.

The creation of Ti_B^+, for example, leads to the formation of a complex in which the Ti atom is surrounded by n=8 hydrogen atoms (4 hydrogen atoms are shared with the neighboring BH_4 unit), the Ti-H distances ranging from 1.72 to 2.25 Å; see Fig. 8(a). Similar lattice rearrangements are seen in the case of Ti_B^- [see Fig. 8(b)] where we also find a complex which can be described as TiH_8 with the Ti-H distances ranging from 1.83 to 2.10 Å.

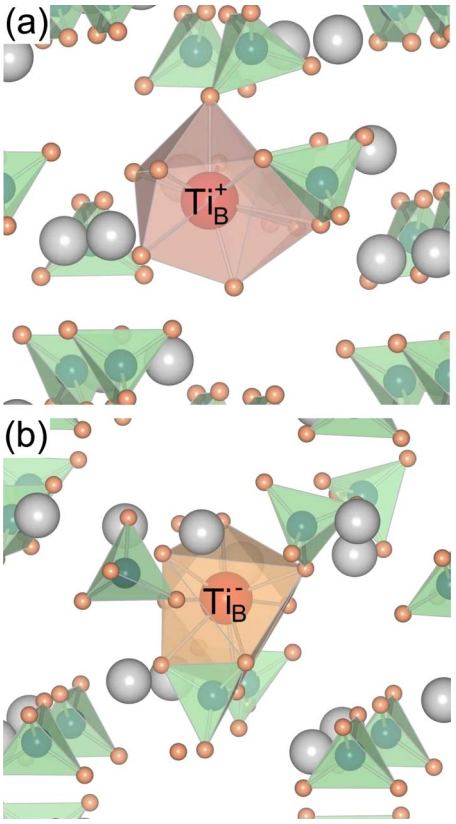

FIG. 8. (Color online) Lattice relaxations induced by (a) Ti_B^+ and (b) Ti_B^- in $LiBH_4$. Large (gray) spheres are Li, medium (blue) spheres B, and small (orange) spheres H. The impurity atom (large red sphere) tends to pull hydrogen atoms from the neighboring BH_4 units to form a metal-hydrogen complex.

Although a precise determination of n for MH_n complexes depends on the chosen cutoff for the M-H distance, there is a tendency for n to have larger values in cases where the transition-metal impurities have a larger number of empty d states (such as Ti and Zr). Experimentally, additives such as TiO_2, $TiCl_3$, and ZrO_2 were found to effectively reduce the dehydrogenation temperature and improve the reversibility of $LiBH_4$, but they were also found to reduce the hydrogen storage capacity.[30] This may partly be caused by the formation of MH_n complexes (M=Ti and Zr) observed in our studies.

B. $Li_4BN_3H_{10}$

Table II summarizes the results for transition-metal impurities in $Li_4BN_3H_{10}$. Again, we list the transition level $\varepsilon(+/-)$ between charge states +1 and −1, the associated U value, and the corresponding formation energy E_f of the different impurities on the B, N, and Li sites, and at interstitial sites. Like in $LiBH_4$, all the impurities nominally on the B site in $Li_4BN_3H_{10}$ have negative U values.

For transition-metal impurities on the N and Li sites, negative U values are found as well, except for Zr_N, Fe_N, and Ni_{Li}. Interstitial sites, on the other hand, generally yield positive U values, except for Zr_i (which, however, has high formation energy and is thus unlikely to incorporate in this

TABLE II. Transition level $\varepsilon(+/-)$ between charge states +1 and −1, the associated U value, and the corresponding formation energy E^f (where U is negative) of different impurities at the B, N, and Li sites, and at interstitial sites in $Li_4BN_3H_{10}$. In cases where U is positive, E^f is the formation energy of impurities in the neutral charge state. Configurations that have positive U but may still be effective in shifting the Fermi level are marked by a $\surd$ sign, whereas ineffective configurations are marked with a × sign. Work functions (Φ) of the impurities in their metallic states are also given for reference. All the quantities are given in electron volt (eV). The transition level between H_i^+ and H_i^- (in their most stable configurations) is at $\mu_e^{int}=2.61$ eV.

		Ti	Zr	Fe	Ni	Pd	Pt	Zn
	Φ [a]	4.10	4.00	4.65	5.15	5.00	5.40	4.30
B site	$\varepsilon(+/-)$	3.12	3.18	2.25	1.91	1.82	1.78	1.92
	U	−2.16	−0.27	−0.30	−1.30	−2.62	−2.26	−3.65
	E^f	1.10	0.98	0.86	0.31	−0.12	−0.82	0.02
	$\varepsilon(+/-)-\mu_e^{int}$	+0.51	+0.57	−0.36	−0.70	−0.79	−0.83	−0.69
N site	$\varepsilon(+/-)$	3.73	3.60	3.04	2.52	2.15	2.21	2.77
	U	−0.12	+0.39	+0.25	−1.18	−1.76	−1.99	−1.26
	E^f	5.06	4.96	4.58	2.73	2.05	1.61	2.92
	$\varepsilon(+/-)-\mu_e^{int}$	+1.12	$\surd$	$\surd$	−0.09	−0.46	−0.40	+0.16
Li site	$\varepsilon(+/-)$	2.82	2.80	2.82	1.87	1.73	1.84	3.21
	U	−1.60	−1.97	−0.23	+0.20	−0.86	−1.18	−1.09
	E^f	2.07	2.05	4.01	2.79	2.66	2.55	2.82
	$\varepsilon(+/-)-\mu_e^{int}$	+0.21	+0.19	+0.21	$\surd$	−0.88	−0.77	+0.60
Interstitial	$\varepsilon(+/-)$	3.82	3.23[b]	2.63[c]	2.61	2.35	2.16	2.65
	U	+0.15	−0.37	+0.27	+2.54	+3.12	+2.42	+2.18
	E^f	4.41	4.21	3.72	1.67	1.31	1.66	2.09
	$\varepsilon(+/-)-\mu_e^{int}$	$\surd$	+0.62	×	×	×	×	$\surd$

[a]Reference 29.
[b]Zr_i^+ and Zr_i^- are not most stable among possible charge states of the Zr interstitial. Zr_i^{2+} and Zr_i^{2-}, are lower in energy, yielding a negative-U impurity with $\varepsilon(2+/2-)=3.15$ eV (corresponding to $E_f=4.11$ eV).
[c]Fe_i^+ and Fe_i^- are not most stable among possible charge states of the Fe interstitial. Fe_i^{2+} and Fe_i^{2-}, are lower in energy, yielding $\varepsilon(2+/2-)=2.68$ eV with a very small positive U.

form). Many of the impurities on the N and Li sites and at interstitial sites in $Li_4BN_3H_{10}$ have higher formation energies than those nominally on the B site (with respect to the chosen set of chemical potentials). The formation energies of Ni, Pd, and Pt on interstitial sites are quite low but these interstitials are expected not to be effective in $Li_4BN_3H_{10}$ (see below).

As we have discussed in the previous section, impurities with positive-U character can still be effective in shifting the Fermi level, depending on the relative position of $\varepsilon(+/0)$, $\varepsilon(0/-)$, and μ_e^{int}. Among the impurities with positive-U character in $Li_4BN_3H_{10}$, Ni_{Li} gives $\varepsilon(0/-)<\mu_e^{int}$, whereas Zr_N, Fe_N, Ti_i, and Zn_i have $\varepsilon(+/0)>\mu_e^{int}$; as far as the transition level is concerned, these impurities may still be effective in shifting the Fermi level. Others such as Fe_i, Ni_i, Pd_i, and Pt_i are expected not to be effective because the transition levels of these impurities are such that $\varepsilon(+/0)<\mu_e^{int}<\varepsilon(0/-)$.

Lattice relaxations of $Li_4BN_3H_{10}$ are also very significant in the presence of these impurities. Again, the impurities tend to pull other BH_4 closer, and/or break B-H bonds to form MH_n complexes. In addition, the interaction between the transition metals and $Li_4BN_3H_{10}$ also leaves the systems with an NH_3 molecule in the case of positively charged Pd, Pt, and Zn impurities on the B site. Substitution of a nitrogen atom in $Li_4BN_3H_{10}$ by a transition-metal impurity M leaves the system with an MH_2 unit, usually a quasilinear H-M-H. The value of the H-M-H angle in an MH_2 unit depends on the specific impurity and its charge state.

C. Trends and discussion

We now try to identify trends among different metallic impurities in $LiBH_4$ and $Li_4BN_3H_{10}$ and possible correlations between different physical quantities. Figure 9 shows one attempt at establishing trends and correlations by analyzing band lineups and positions of the $\varepsilon(+/-)$ level for different transition-metal impurities nominally on the B site. The band structures of $LiBH_4$ and $Li_4BN_3H_{10}$ were aligned assuming that the universal alignment of the transition level between H_i^+ and H_i^- (at 4.5 eV below the vacuum level) holds true in these compounds.[31]

As mentioned above, lattice relaxations in these complex hydrides (containing light elements) are very large and the impurities create different patterns in the lattice geometry of the doped systems depending on charge states of the dopants. In addition, these impurities can interact with many hydrogen atoms via their d states.

For many of the impurities, the position of the transition

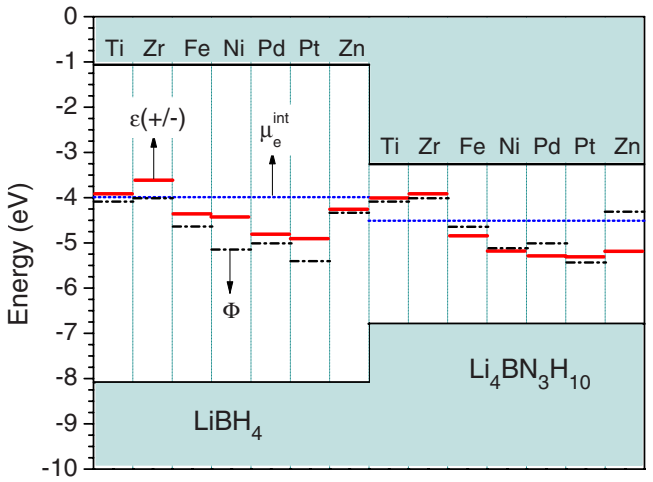

FIG. 9. (Color online) Band lineups and position of the $\varepsilon(+/-)$ levels (thick red lines) for different transition-metal impurities nominally on the B site. Band structures of $LiBH_4$ and $Li_4BN_3H_{10}$ are aligned assuming the universal alignment of the transition level between H_i^+ and H_i^- (Ref. 31). Work functions (Φ) of the impurities in their standard metallic states are marked by the (black) dash-dotted lines; μ_e^{int} levels are presented by the (blue) dotted lines.

levels $\varepsilon(+/-)$ *qualitatively* follows the same trend as the work function values of the corresponding elemental transition metals. However, there is no direct quantitative correlation, presumably due to the intricacies of the interactions between transition-metal *d* states and hydrogen. The transition level $\varepsilon(+/-)$ moves up in going from Ti to Zr, moves down in going from Ni→Pd→Pt, and moves down in going from Ti→Fe→Ni. Zn may behave differently from Ti, Fe, and Ni because unlike these transition metals, Zn has a completely filled *d* shell.

Zn also behaves differently in different compounds. For example, the creation of Zn_B^+ in $LiBH_4$ leaves the system with a trigonal planar ZnH_3 complex sharing one H atom with its neighboring BH_4 unit (alternatively, a ZnH_2-H-BH_3 complex) plus an H_2 molecule, whereas in $Li_4BN_3H_{10}$ it produces a trigonal planar ZnH_3 complex plus a NH_3 unit. Given the fact that Zn_B^- creates a ZnH_4 unit in both compounds, the different relaxation patterns of Zn_B^+ may explain why the transition level $\varepsilon(+/-)$ of Zn in $Li_4BN_3H_{10}$ is much lower than its work function, unlike in $LiBH_4$ (see Fig. 9).

VI. COMPARISON WITH EXPERIMENT

Finally, we check the correlation between our results and what is known experimentally. In $LiBH_4$, Ti and Zn have experimentally been found to be effective in enhancing kinetics while Fe was found to be ineffective.

For Ti, our results show that incorporation of the impurity is about equally favorable on the Li site, the B site, or at interstitial sites; all would lead to a shift in the Fermi level μ_e^{int}. The shift is largest for the interstitial position. Zn will also be effective, if incorporated on the B site. In the case of Fe, which according to our calculations could potentially incorporate on the B site and have a positive effect there. Experimentally, however, Fe is found to be ineffective. One possible explanation for this is that we have not yet investigated all possible interactions between the impurities and the host constituents. If a particularly stable phase would form between Fe and any of the host constituents (or other elements in the precursors), its incorporation could be hampered.

From the results presented in Table I, we expect that Zr, Ni, Pd, and Pt (if incorporated on the B or Li site), like Ti and Zn, may also be effective in enhancing the kinetics of $LiBH_4$. Besides, since Ni, Pd, and Pt can shift the Fermi level to lower values (see Table I), they increase the formation energy of V_H^- (while decreasing that of V_H^+) and hence reduce the number of BH_3 units associated with its formation. As a result, they may help reduce boron loss caused by diborane emission.

In $Li_4BN_3H_{10}$, Ni, Pd, and Pt have experimentally been found to be effective while Ti, Fe, and Zn were found not to be effective. From our computational work, it immediately jumps out that Ni, Pd, and Pt all have very low formation energies when incorporated on the B site. And when incorporated on that site, Ni, Pd, and Pt all give rise to large Fermi-level shifts, thus facilitating the formation of hydrogen-related defects. In addition, these impurities can also be very effective in shifting the Fermi level if incorporated on the N and Li sites. This provides a gratifying correlation with experiment.

As for the impurities that experimentally been found to be ineffective, we find Ti and Fe to have significantly higher formation energies than Ni, Pd, or Pt; hence they are less likely to incorporate and affect the kinetics. Even when incorporated (which would be easiest on the B site), these impurities would give rise to smaller shifts in the Fermi level compared to Ni, Pd, and Pt, and hence be less effective.

Similar to the case of Fe in $LiBH_4$, while Zn is found to be potentially effective in $Li_4BN_3H_{10}$ according to our calculations, experiments found it to be ineffective. One possible explanation is the formation of stable zinc hydride phase(s) and ammonia as suggested by our calculations (see Sec. V C).

VII. SUMMARY

In summary, our first-principles studies show that hydrogen-related defects in $LiBH_4$ and $Li_4BN_3H_{10}$ are positively and negatively charged and their formation energies are, therefore, Fermi-level dependent. One can tailor the formation energies of these native point defects (hence the kinetics of the system) by shifting the Fermi level. This can be accomplished by adding appropriate impurities, which are electrically active, into the systems. We found that a number of transition-metal impurities are effective in shifting the Fermi level of $LiBH_4$ and $Li_4BN_3H_{10}$. Different impurities in different configurations, however, produce shifts of different magnitudes (or do not shift the Fermi level at all).

The comprehensive results that we have obtained to date are in qualitative agreement with experimental observations, in that they indeed show an expected enhancement in kinetics for some impurities that have experimentally been found

to be effective. The lack of enhancement for impurities that have been found to be ineffective can also be understood in terms of our results. In addition, based on our analysis of the lattice relaxations in $LiBH_4$ induced by hydrogen-related defects and impurities, we have proposed possible explanations for the unrecoverable loss of boron during dehydrogenation process and for the reduced hydrogen storage capacity reported experimentally.

The purpose of our studies is, of course, not simply to reproduce experiment. The correlation that is being demonstrated here provides support for our proposed model, namely, that the enhancement in kinetics is directly tied to the specifics of the electrical activity of the impurities. As such, we can provide an explanation for the observed effects, and a foundation for tailored efforts to improve the performance of existing materials or design new materials.

ACKNOWLEDGMENTS

The authors acknowledge support by General Motors Corporation and helpful discussions with J. Herbst and A. Janotti. This work made use of NERSC resources supported by the DOE Office of Science under Contract No. DE-AC02-05CH11231 and of the CNSI Computing Facility under NSF Grant No. CHE-0321368.

*Corresponding author; vandewalle@mrl.ucsb.edu

[1] L. Schlapbach and A. Züttel, Nature (London) **414**, 353 (2001).
[2] M. S. Dresselhaus and I. L. Thomas, Nature (London) **414**, 332 (2001).
[3] J. Hafner, C. Wolverton, and G. Ceder, MRS Bull. **31**, 659 (2006).
[4] A. Züttel, S. Rentsch, P. Fischer, P. Wenger, P. Sudan, Ph. Mauron, and Ch. Emmenegger, J. Alloys Compd. **356-357**, 515 (2003).
[5] G. P. Meisner, M. L. Scullin, M. P. Balogh, F. E. Pinkerton, and M. S. Meyer, J. Phys. Chem. B **110**, 4186 (2006).
[6] F. E. Pinkerton, M. S. Meyer, G. P. Meisner, and M. P. Balogh, J. Phys. Chem. B **110**, 7967 (2006).
[7] A. Peles and C. G. Van de Walle, Phys. Rev. B **76**, 214101 (2007).
[8] M. Au, A. R. Jurgensen, W. A. Spencer, D. L. Anton, F. E. Pinkerton, S.-J. Hwang, C. Kim, and R. C. Bowman, Jr., J. Phys. Chem. C **112**, 18661 (2008).
[9] X. B. Yu, D. M. Grant, and G. S. Walker, J. Phys. Chem. C **112**, 11059 (2008).
[10] F. E. Pinkerton, M. S. Meyer, G. P. Meisner, and M. P. Balogh, J. Alloys Compd. **433**, 282 (2007).
[11] C. G. Van de Walle and J. Neugebauer, J. Appl. Phys. **95**, 3851 (2004).
[12] J. F. Herbst and L. G. Hector, Jr., Appl. Phys. Lett. **88**, 231904 (2006).
[13] J. P. Perdew, K. Burke, and M. Ernzerhof, Phys. Rev. Lett. **77**, 3865 (1996).
[14] P. E. Blöchl, Phys. Rev. B **50**, 17953 (1994).
[15] G. Kresse and D. Joubert, Phys. Rev. B **59**, 1758 (1999).
[16] G. Kresse and J. Hafner, Phys. Rev. B **47**, 558 (1993).
[17] G. Kresse and J. Furthmüller, Phys. Rev. B **54**, 11169 (1996).
[18] G. Kresse and J. Furthmüller, Comput. Mater. Sci. **6**, 15 (1996).
[19] H. J. Monkhorst and J. D. Pack, Phys. Rev. B **13**, 5188 (1976).
[20] J.-Ph. Soulié, G. Renaudin, R. Černý, and K. Yvon, J. Alloys Compd. **346**, 200 (2002).
[21] J. B. Yang, X. J. Wang, Q. Cai, W. B. Yelon, and W. J. James, J. Appl. Phys. **102**, 033507 (2007).
[22] D. J. Siegel, C. Wolverton, and V. Ozoliņš, Phys. Rev. B **75**, 014101 (2007).
[23] K. Miwa, N. Ohba, S. I. Towata, Y. Nakamori, and S. I. Orimo, Phys. Rev. B **69**, 245120 (2004).
[24] Z. Łodziana and T. Vegge, Phys. Rev. Lett. **93**, 145501 (2004).
[25] L. G. Hector, Jr. and J. F. Herbst, J. Phys.: Condens. Matter **20**, 064229 (2008).
[26] G. D. Watkins, in *Festkörperprobleme: Advances in Solid State Physics*, edited by P. Grosse (Vieweg, Braunschweig, 1984), Vol. 24, p. 163.
[27] Z. Łodziana, A. Züttel, and P. Zielinski, J. Phys.: Condens. Matter **20**, 465210 (2008).
[28] G. Henkelman, B. P. Uberuaga, and H. Jónsson, J. Chem. Phys. **113**, 9901 (2000).
[29] J. A. Dean, *Lange's Handbook of Chemistry*, 14th ed. (McGraw-Hill, New York, 1992).
[30] M. Au and A. Jurgensen, J. Phys. Chem. B **110**, 7062 (2006).
[31] C. G. Van de Walle and J. Neugebauer, Nature (London) **423**, 626 (2003).